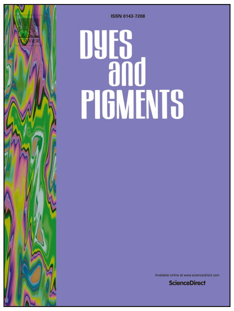

Aggregation-induced emission organogel formed by both sonication and thermal processing based on tetraphenylethylene and cholesterol derivative

Miao Luo, Sheng Wang, Chengpeng Li, Wangen Miao, Xiang Ma

PII: S0143-7208(18)32870-5
DOI: https://doi.org/10.1016/j.dyepig.2019.02.041
Reference: DYPI 7375

To appear in: *Dyes and Pigments*

Received Date: 28 December 2018
Revised Date: 15 February 2019
Accepted Date: 23 February 2019

Please cite this article as: Luo M, Wang S, Li C, Miao W, Ma X, Aggregation-induced emission organogel formed by both sonication and thermal processing based on tetraphenylethylene and cholesterol derivative, *Dyes and Pigments* (2019), doi: https://doi.org/10.1016/j.dyepig.2019.02.041.

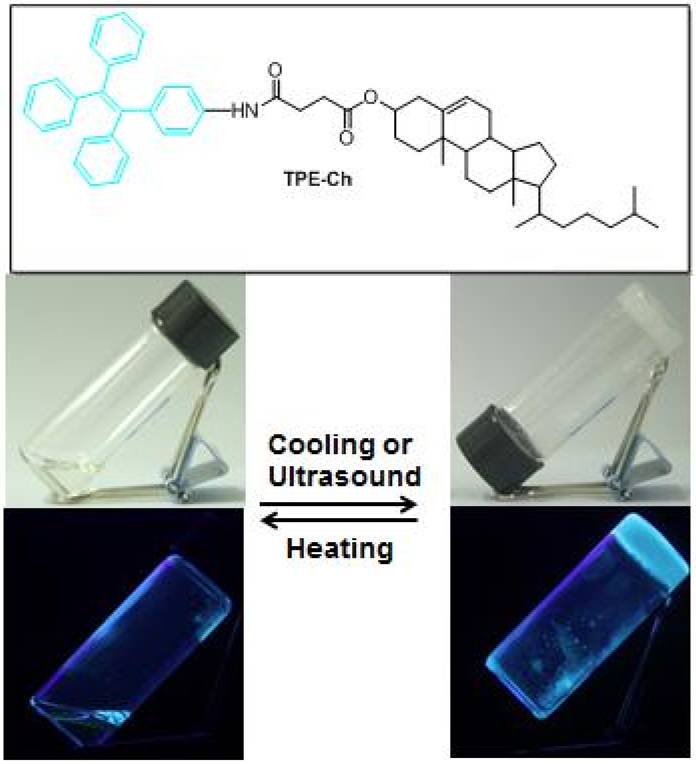
HN
O
O
O
TPE-Ch
Cooling or
Ultrasound
Heating

Aggregation-induced emission organogel formed by both sonication and thermal processing based on tetraphenylethylene and cholesterol derivative

Miao Luo,[a] Sheng Wang,*[a] Chengpeng Li,[a] Wangen Miao,[a] and Xiang Ma*[b]

[a] College of Basic Education, School of Chemistry and Chemical Engineering,
Lingnan Normal University, Zhanjiang Preschool Education College, Zhanjiang,
524037, Guangdong, P. R. China
[b] Key Laboratory for Advanced Materials and Institute of Fine Chemicals, East China
University of Science and Technology
Meilong Road 130, Shanghai, 200237, P. R. China

**Corresponding author: Prof. Dr. Sheng Wang, College of Chemistry Science & Technology, Lingnan Normal University, Zhanjiang 524048, P.R. China; Tel: +86-759-318-2515; Fax: +86-759-318-3510; E-mail: dyesws@126.com;*
Prof. Dr. Xiang Ma, Key Laboratory for Advanced Materials and Institute of Fine Chemicals, East China University of Science and Technology
Meilong Road 130, Shanghai, 200237, P. R. China; Tel: +86-21-64252288, Fax: +86-21-64252288; E-mail: maxiang@ecust.edu.cn

Abstract： In this work, we designed and synthesized a novel asymmetric tetraphenylethylene-based fluorescence compound, which can form cholesteryl liquid crystal by cooling from the isotropic melt and exhibit typical AIE property with a 180-fold enhancement of fluorescence intensity in 90% water fraction of THF/water mixture than pure THF. This compound can gelate in cyclohexane via both ultrasound stimuli and general sol–gel processes accompanied by remarkable enhanced fluorescence emission. The self-assembly and gelling properties can be controlled by ultrasound stimuli and renewed by a thermodynamic process. The mechanism of the process was investigated by UV-Vis absorption, PL emission, scanning electron microscopy, wide-angle X-ray scattering analysis, and small-angle X-ray scattering analysis. The results reveal that the cooperation and relative competition of multiple intermolecular interactions, which are the main contributors for the formation of gel influenced by the sonication or thermal stimulus.

Keywords: *aggregation-induced emission, tetraphenylethylene derivatives, organogelator, gelation-induced fluorescence enhancement, liquid crystal*

1. Introduction

Research on organic luminescent materials has attracted numerous attentions because of their vast potential in fluorescent sensors, organic electronics, optoelectronics, and light-emitting diode fabrication.[1-3] However, conventional fluorescent molecules containing large planar aromatic rings often suffer from aggregation-caused quenching (ACQ) due to their intermolecular π-π interactions in the aggregate state or solid state, which will limit their developments and applications in fluorescent chemosensors, bioprobes, light detectors, organic light-emitting devices (OLEDs), etc.[1, 2, 4] Promisingly, the aggregation-induced emission (AIE) effect, which is opposite to the ACQ phenomenon, was first reported by Tang and co-workers in 2001. [5] Excitingly, many organic dyes with aggregation-induced emission (AIE) characteristics have been found successively.[1, 6-10]

In recent years, aggregation-induced emission (AIE) organogelators, which exhibited remarkable variation in the fluorescence spectrum accompanying a gel-to-sol or sol-to-gel phase transition process, have received much attention from both theoretical and practical viewpoints.[3, 11-27] For example, Park and coworkers synthesized a novel fluorescent molecule, 1-cyano-trans-1, 2-bis-(3’, 5’-bis-trifluoro-methyl-biphenyl)ethylene (CN-TFMBE) without long alkyl chain or steroidal substituents, showed a typical aggregation-induced enhanced emission (AIEE) phenomenon.[25] Ihara and Lu reported a new organogelator based on a salicylideneaniline derivative with cholesterol units, exhibited strong fluorescence enhancement in the gel state relative to a solution of the same concentration because of the formation of J aggregations.[26]

Recently, stimuli-responsive low-weight molecular organogels (LMOGs) has been studied extensively in areas ranging from chemistry and biology to materials science because of their potential applications in drug delivery, sensors, adaptive materials, and nano/micro devices.[28-31] However, most of the reported responsive materials were stimulated by light, reaction, and heat, therefore, a smart gel controlled or even switched by sound is also very appealing.[28] There are some reports recently appeared about the gelation formation by ultrasound stimuli.[28, 29, 32-34] Huang’s group reported a novel family of asymmetric cholesterol-based fluorescent organogelators, their self-assembly and surface wettability can be controlled by ultrasound stimuli and restored by a thermal process.[28, 29]

Thus, combining an AIE luminogen and a stimulus-responsive organogelator would be a promising strategy for constructing smart luminescent systems. In 2016, Srivatsan and coworkers reported a family nucleolipid gels displayed aggregation-induced enhanced emission and their gelation behavior and photophysical properties could be reversibly switched by external stimuli such as temperature, ultrasound and chemicals.[35] However, low-weight molecular organogel reversibly switched by ultrasound and thermal stimuli with aggregation-induced emission property is very rare thus far to the best of our knowledge.[28, 29, 36] It is reported that the balance of the hydrogen-bonds with other interactions (such as hydrophobic interactions and π-π interactions, as well as the steric hindrance) are necessary to satisfy the requirements of ultrasonic stimuli for gelation.[28, 36] Herein, we report a novel AIE compound derived from tetraphenylethylene and cholesterol moieties with the structural character of ALS (aromatic group A, linker L, steroidal group S)[28, 29], the gelling ability, aggregation behavior, and response to ultrasound stimuli are also elucidated.

Scheme 1

2. Experimental

2.1 Materials and instruments

4-Aminophenylboronic acid, 2-bromo-1,1,2-triphenylethylene, cholesterol, succinic anhydride, aliquat 336, tetrakis (triphenylphosphine) palladium (0) were purchased from Aladdin company and used as received. 4-dimethylamiopryidine (DMAP), 1-(3-dimethylaminopropyl)-3-ethylcarbodiimide hydrochloride (EDC-HCl) were purchased from Shanghai Darui company (China) used as received. Ultra-pure water was used in the experiments. Tetrahydrofuran (THF) was distilled from sodium/benzophenone. All other reagents and solvents were purchased as analytical grade from Zhangjiang Kangbai Company (China) and used without further purification. 4-(1,2,2-triphenylvinyl)benzene-amine (**TPE-NH$_2$**)[12] was prepared according to the literature methods.

The IR spectra were measured on a Nicolet-6700 FT-IR spectrometer by incorporating the samples in KBr disks. Proton and carbon nuclear magnetic resonance (^{1}H NMR and ^{13}CNMR) spectra were measured on a Bruker AVANCE III spectrometer [CDCl$_3$, tetramethylsilane (TMS) as the internal standard]. The electronic spray ionization (ESI) high-resolution mass spectra were tested on a HP 5958 mass spectrometer. The SEM images were obtained by using a Hitachi S-4800 spectrometer. The AFM images were obtained by using Veeco/DI Scanning Probe Microscope and the TEM Images by using JEM-1400 Plus (JEOL Ltd., Japan) at 120 kV. The UV/Vis spectra were determined on a Shimadzu-2550 spectrophotometer. Wide-angle X-ray diffraction (WAXD) measurement was performed by using a Philips X’Pert Pro diffractometer with an X-ray source of Cu Ka (λ=0.15406 nm) at 40 kV and 40 mA, at scan rates of 2.4 ° per 1 min. Small-angle X-ray diffraction (SAXD) measurement was performed by using a Rigaku D/max 2550V with an X-ray source of Cu Ka (λ=0.15406 nm) at 40 kV and 100 mA, at scan rates of 0.6^o per 1 min. Canon EOS 60D and EOS 70D digital camera was used to take photographs. The sonication gel (S-gel) was gained by using SK5210HP (Shanghai Kedao Company, working frequency: 53 kHz, ultrasonic power: 200 W, the power can vary from 40% to 100%).

The calculations were performed with the periodic density functional theory (DFT) method using the DMol^3 module in the Materials Studio 7.0 software package.[37]

The DMol^3 calculation: Task: Geometry Optimization; Quality: Medium; Functional: GGA, PW91. Basis set: DND; Basis file: 3.5. The DMol^3 electronic options: SCF tolerance: 1.0 × e^{-5}; Max. SCF cycles: 500.

2.2 Synthesis of 3-Cholesteryloxycarbonylpropanoic acid (1):

A solution of cholesterol (5.80 g, 15 mmol), succinic anhydride (1.50 g, 15 mmol), pyridine (1.00 mL), and dry heptane (150 mL) were heated to reflux for 21 h and cooled to room temperature. The resulting precipitate was recrystallized twice from acetone. Yield: 70%.

2.3 Synthesis of TPE-Ch:

TPE-NH$_2$ (0.30 g, 0.86 mmol) and **1** (0.42 g, 0.99 mmol) were dissolved in THF (50 mL), and then EDC-HCl (0.01 g) and DMAP (0.01 g) were added. The solution was stirred at room temperature for 12 hours. After removing the solvent under reduced pressure, the residue was crystallized from ethanol to give white crystalline powder **TPE-Ch** (0.44 g, 62.8% yield). IR (KBr): υ=3433 cm^{-1}(N-H), 2946 cm^{-1} (-CH$_2$-), 2857 cm^{-1} (-CH$_3$), 1732 cm^{-1} (C=O at COOR), 1698 cm^{-1} (C=O at RCONHR'), 1670 cm^{-1} (C=C), 1597, 1525, 1492 cm^{-1} (phenyl); ^{1}H NMR (400 MHz, CDCl$_3$) δ 7.65 (s, 1H), 7.27 (s, 1H), 7.18 – 6.95 (m,16H), 5.39 (d, *J* = 3.9 Hz, 1H), 4.73 – 4.59 (m, 1H), 2.73 (t, *J* = 6.2 Hz, 2H), 2.62 (t, *J* = 6.3 Hz, 2H), 2.33 (d, *J* = 7.7 Hz, 2H), 2.01 (t, *J* = 16.0 Hz, 2H), 1.85 (t, *J* = 15.8 Hz, 3H), 1.55 – 0.84 (m, 33H), 0.70 (s, 3H); ^{13}C-NMR (CDCl$_3$, 75MHz) δ (ppm):172.8, 169.5, 143.9, 140.6, 140.1, 139.7, 132.1, 131.1, 127.8, 126.2, 122.7, 118.8, 74.5, 56.6, 56.3, 49.8, 42.5, 39.7, 37.8, 36.9, 36.4, 36.1, 35.9, 32.6, 31.6, 29.0, 28.0, 24.3, 23.7, 22.4, 20.9, 19.4, 18.4, 12.1;

MALDI-TOF MS (ES+): m/z 816.53 ([M+H]$^+$, calcd for $C_{57}H_{69}NO_3$, 815.53).

3. Result and discussion

3.1 Synthesis

The target compound was synthesized according to the routes depicted in Scheme 1. The molecular structure of the target compound with the structural character of ALS (aromatic group A, linker L, steroidal group), in which a tetraphenylethylene (TPE) unit was used as aromatic group A and cholesterol was used as steroidal group S. The TPE core, a propeller-like luminogen, as a prototypical AIEgen, is expected to make the molecule display aggregation-induced emission.[2, 6, 13, 38, 39] Cholesterol is favorable for facilitating gelation of solvents and thus been widely used for designing new LMOGs.[18, 19] The TPE group and cholesterol group were linked by an alkyl chain with an acyl amino linkage. Therefore, it can be expected that three kinds of intermolecular interactions, including hydrogen bonding, π-π interactions, and hydrophobic interactions, would be involved in the formation of the gelation process. Their molecular structures were confirmed by ^{1}H and ^{13}C NMR spectroscopy, mass spectrometry (MS) and Fourier-transform infrared spectroscopy (FT-IR).

3.2 AIE properties

The UV-Vis absorption and PL emission behaviors of the diluted mixtures of the compound were studied in a mixture of THF/water with different water fractions to determine their AIE properties. The PL spectra of 2.5×10^{-5}M compound **TPE-Ch** in THF/water mixtures with different water contents was shown in Figure 1. The figure shows that the PL intensity was very weak and essentially did not change as the water fraction of the THF/water mixture increased from 0% to 80%.Very interesting, a dramatic enhancement in luminescence was observed when the water fraction reached 90%, which was approximately 180 times higher than that in the pure THF. This result indicated that this compound exhibited strong AIE activity. The AIE activity may be attributed to the restriction of intramolecular rotations (RIR) of the tetraphenylethylene (TPE) when in aggregation state.[9]

Figure 1

The UV-vis absorption spectra of compound **TPE-Ch** in the THF/water mixtures (2.5×10^{-5}M) are shown in Figure S1. The spectra displayed absorption tails extending well into the long wavelength region, indicating that the molecules aggregated into nanoparticles in the mixtures. The Mie effect of the nanoparticles has been considered to cause such leveling-off of tails in the absorption spectra. [12, 39, 40]Therefore, the increase in PL intensity can be attributed to an AIE effect caused by the formation of molecular aggregates, in which the restriction of intramolecular rotations increased the fluorescent emission.

Quantum mechanical computations were conducted using the Materials Studio 7.0 software to study the lowest energy spatial conformation of the compound.[6] The energy of the molecule with different conformation was calculated by GGA/PW91 method. The highest occupied molecular orbitals (HOMOs) and the lowest unoccupied molecular orbitals (LUMOs) of the compound were obtained (Figure 2) after structural optimization. As shown in Figure 2, the electron cloud distributions in HOMO and LUMO of **TPE-Ch** was mainly localized on the tetraphenylethylene and the amide moieties with the energy gap between the HOMO and LUMO of 0.79 ev.

Figure 2

3.3 Gelation property

The gelation tests on **TPE-Ch** were carried out in various solvents with 3.0% (w/v) as a standard concentration by using a test-tube-inversion method[29]. (Table 1) A mixture **TPE-Ch** and solvent was heated until the solid was dissolved. A thermodynamic gel (T-gel) was obtained after the hot solution had been cooled to room temperature and aged for at least 30 min. A sonication gel (S-gel) was identified when the hot solution was allowed to cool to room temperature (25^{o}C) and was treated immediately with ultrasound (200 W, 53 kHz, 25^{o}C).[28, 29] The gelation was then checked visually at about 25^{o}C (Figure 3).

Table 1

Figure 3

It is interesting to note that gelation occurred in cyclohexane solution of **TPE-Ch** by ultrasonic treatment (200 W, 53 kHz) for 5 minutes (designated as S-gel). To our surprise, **TPE-Ch** could also form gel by directly cooling the hot solution (above 75 ^{o}C) to room temperature and aging for about 30 min (designated as T-gel). The critical gelation concentration (CGC) (tested by using the "stable to inversion of a test tube" method[41]) was significantly decreased from 60 mg mL^{-1} in the cooling process to 17 mg mL^{-1} in the ultrasonic process, and the gel–sol transition temperature (T_g) (determined by the"falling drop" method[20]) of S-gel was higher than that of the T-gel for the same concentration. (Table 2) In addition, the power and the concentration can influence the time to form the S-gel. The stronger the power was, the shorter the time needed to form the S-gel. The higher the concentration was, the shorter the time needed to form the S-gel, too.(Figure 4) At the same time, after undergoing sonication, a reversed gel (R-gel) was obtained by heating the S-gel to a sol and then cooling it to room temperature.

Table 2

Figure 4

The gelator was found to be initially insoluble in these solvents at room temperature, but the mixtures became clear after heating. Upon cooling or ultrasonic process of these solutions to room temperature, the formation of immobile gels was observed. This thermo-reversible gelation process, which is characteristically accompanied by enhanced fluorescence emission, can easily be distinguished even by naked eyes from the photographic images (in Figure 5A).

To investigate the interrelationship between the emission and aggregation modes along with the sol-gel transition, the temperature dependent fluorescence spectra in the cyclohexane (60 mg mL^{-1}) was measured from 70 to 25 ^{o}C. As shown in Figure 5B, the initial solution exhibited almost non-fluorescence, but the fluorescence intensity increased along with the decrease in temperature. The remarkable fluorescence enhancement from the gels was possibly due to the formation of self-assembly aggregates belonged to gelation-induced fluorescence enhanced emission.[42]

Figure 5

In order to gain better insight into the molecular organization in the gel specimens, the morphologies of xerogels obtained from **TPE-Ch** were investigated by scanning electron microscopy (SEM), Atomic Force Microscope (AFM) and Transmission electron microscope (TEM) (Figure 6, Figure S2). Interestingly, we found that the morphologies of **TPE-Ch** xerogels strongly depend on external stimuli. The T-gel xerogel of cyclohexane generated the formation of sheets consisting of porous aggregates, while tightly arranged three-dimensional branch-like fibers of approximate width 100 nm to form entangled networks were obtained from the S-gel. Furthermore, the morphology of such a gel from sonication showed rod-like structure of several micrometres and curled sheets changed by a sol–gel process(R-gel). The results strongly suggest that the sonication has changed the aggregation action in the process of gelation. The morphology of the gel observed by AFM and TEM was in agreement with the SEM analysis.

Figure 6

The compound **TPE-Ch** exhibited similar absorption spectra for the S-gel, T-gel and R-gel, particularly, the maximum absorption in **TPE-Ch** in THF solution (2.5×10^{-5} mol L^{-1} was located at 318 nm and 253 nm in the gel (6.8×10^{-2} mol L^{-1}), irrespective of sonication or cooling (Figure S3), The blueshifted absorption indicated an H aggregation of **TPE-Ch** molecules in the gel.[28] The emission of S-gel occurred at 477 nm was shifted to 470 nm for the T-gel and R-gel, respectively (Figure 7). The redshift of the emission in the S-gel with respect to that in T-gel and R-gel suggested the sonication treatment may strengthen the π-π interaction.[29]

Figure 7

To check the contribution of hydrogen bonds in the amide and ester groups to the gelation process, the infrared spectra of TPE-Ch before and after gelation were measured, and the NH stretching bands ($υ_{NH}$) and C=O stretching bands ($υ_{C=O}$) were carefully examined(Figure 8). The results were summarized in Table 3. The sample before gel showed a relatively weak NH stretching band at 3413 cm^{-1} and a weak C=O stretching band at 1733 cm^{-1}.However, the gel samples of T-gel and R-gel showed a strong NH stretching band at 3331 cm^{-1} and a strong C=O stretching band at 1733 cm^{-1} for intermolecular hydrogen bonding. Moreover, in the S-gel sample of **TPE-Ch**, the NH stretching bands at 3433 and 3343cm^{-1} also indicates the existence of hydrogen bonding in the S-gel.[43] The NH stretching bands were obviously blueshifted compared with the T-gel and the R-gel, which suggests that the sonication may releases the self-lock and induces the formation of semistable initial aggregates, leading to accelerated gelation rates and formation of higher-order nanostructures.[28, 29, 32, 34]

Table 3

Figure 8

The molecular packing of the **TPE-Ch** xerogels under different external stimuli was further investigated by powder X-ray diffraction spectra (Figure 9). For SAXD, the neat solid of **TPE-Ch** showed peak at 2.52 corresponding to *d* spacing of 3.50 nm, and the T-gel xerogel and S-gel xerogel of **TPE-Ch** displayed similar X-ray diffraction profiles, with two peaks corresponding to *d* spacings of 5.58 nm, 2.68 nm and 5.25 nm, 3.11 nm, respectively, these values indicate that T-gel may form a lamellar structure.[28, 43, 44] The two peaks for the R-gel xerogel correspond to 5.48 nm and 2.74 nm, similar to those of the T-gel xerogel. From WAXD, T-gel and R-gel displayed similar X-ray diffraction profiles at the peak about 0.52 nm, but the neat solid and S-gel showed another peak corresponding to *d* spacing of 0.45 and 0.43 nm, respectively. It is suggested that the aggregation depends on the gelling stimuli and can be recovered without noticeable changes.[28]

Figure 9

On the basis of the spectral study and XRD results, combined with the CPK model of **TPE-Ch**, the molecular packing of the xerogels was conjectured as shown in Figure 10. In the thermal process, the gradual formation of the intermolecular H bonds takes place at amide group and the tetraphenylethylene (TPE) units are packing by face-to-face. The molecules are further connected in the direction perpendicular to the intermolecular H bonds through van der Waals forces between the cholesterol groups with a resulting layer distance of 5.58 nm (structure B in Figure 10). However, in the sonication process, the **TPE-Ch** molecule unwind, as a result, the intermolecular H bonds takes place between NH(amide) and C=O(ester) groups, and the tetraphenylethylene (TPE) units are packing by side-by-side (structure C in Figure 10). It may be the reason that sonication provides heat and pressure on the nanosecond scale and extreme cooling rates, leading to rapid and spontaneous aggregation through interpenetrating H-bond interactions.[28]

Figure 10

3.4 Mesomorphic behavior

The mesomorphic behavior of **TPE-Ch** was evaluated using differential scanning calorimetry (DSC) and hot-stage polarized optical microscopy (POM). Figure 11 shows the first heating, cooling and second heating DSC curves of **TPE-Ch**. For the first heating curve, the lower peak temperature at 126 ^{o}C was the transition between crystalline solid phase and liquid crystalline (LC) phase, and the other transition at 184 ^{o}C belonged to liquid crystalline phase to isotropic phase transition, while a significant cold crystallization at 154 ^{o}C was possibly one liquid crystalline phase to the other crystalline phase transition. The POM observations showed that by heating the temperature above 126 ^{o}C, the sample began to flow with color birefringence, suggestive of a liquid, indicating the sample really turned into the liquid crystalline state. According to the textures obtained during cooling from the isotropic melt and observed by POM (Figure 12), the fingerprint texture formed from **TPE-Ch** may belong to the cholesteryl liquid crystal. The results of DSC and POM studies showed that the characteristics of the phase transitions observed in the DSC curves for **TPE-Ch** are consistent with those found by POM observations

Figure 11

Figure 12

3.5 Thermal property

The thermal property of TPE-Ch was investigated by thermogravimetric analysis (TGA). TPE-Ch exhibited high thermal stability. The decomposition temperature with 5% weight loss under a N_2 atmosphere (5% T_d) was 286.5 ^{o}C.

Figure 13

4. Conclusion

In summary, a novel gelation-induced enhanced emission compound **TPE-Ch** based on tetraphenylethylene and cholesterol derivative has been designed and synthesized. The compound exhibits AIE behavior, as indicated by the significant fluorescence enhancement in the aggregated state and gel state. Moreover, the fluorescence intensity can be reversibly changed with gel-solution transition by alternate cooling and heating. Furthermore, it is surprising that the self-assembly of the compound can be controlled by ultrasound stimuli and restored by a thermal process through intermolecular H bonds, π-π interaction and van der Waals forces. The POM and DSC studies revealed that **TPE-Ch** can form cholesteryl liquid crystal by cooling from the isotropic melt. The self-assembly controlled by the sonication or thermal process may have potential applications in biodelivery systems, responsive materials and etc.

Acknowledgements

This work was financially supported by NSFC (2187080411, 21372194, 21722603 and 21773103). M. Luo also acknowledge the Research Funds of Lingnan Normal University (QL1515) and Zhanjiang Science and Technology Tackling Project(2016B01040).

Reference

[1] Xu F, Yuan M-S, Wang W, Du X, Wang H, Li N, et al. Symmetric and unsymmetric thienyl-substituted fluorenone dyes: static excimer-induced emission enhancement. RSC Adv 2016;6(80):76401-8.

[2] Zhang Y, Mao H, Kong L, Tian Y, Tian Z, Zeng X, et al. Effect of E/Z isomerization on the aggregation-induced emission features and mechanochromic performance of dialdehyde-substituted hexaphenyl-1,3-butadiene. Dyes and Pigments. 2016;133:354-62.

[3] Ren YY, Wu NW, Huang J, Xu Z, Sun DD, Wang CH, et al. A neutral branched platinum-acetylide complex possessing a tetraphenylethylene core: preparation of a luminescent organometallic gelator and its unexpected spectroscopic behaviour during sol-to-gel transition. Chemical communications 2015;51(82):15153-6.

[4] Shanmugasundaram M, Joseph J, Ramaiah D. Tuning of photoluminescence properties of functional phthalides for OLED applications. Journal of Photochemistry and Photobiology A: Chemistry 2016;330:156-62.

[5] Luo J, Xie Z, Lam JWY, Cheng L, Tang BZ, Chen H, et al. Aggregation-induced emission of 1-methyl-1,2,3,4,5-pentaphenylsilole. Chem Commun 2001(18):1740-1.

[6] He Z, Shan L, Mei J, et al. Aggregation-induced emission and aggregation-promoted photochromism of bis(diphenylmethylene)dihydroacenes. Chem Sci 2015;6:3538–43.

[7] Mei J, Leung NLC, Kwok RTK, Lam JWY, Tang BZ. Aggregation-Induced Emission: Together We Shine, United We Soar! Chem Rev 2015;115(21):11718-940.

[8] Liu G, Wu D, Liang J, Han X, Liu SH, Yin J. Tetraphenylethene modified [n]rotaxanes: synthesis, characterization and aggregation-induced emission behavior. Organic & biomolecular chemistry 2015;13(13):4090-100.

[9] Qin A, Tang B. Aggregation-Induced Emission: Fundamentals. Wiley 2014:1-414.

[10] Qin A, Tang B. Aggregation-Induced Emission:Applications. Wiley 2013:1-275.

[11] Yan N, He G, Zhang H, Ding L, Fang Y. Glucose-based fluorescent low-molecular mass compounds: creation of simple and versatile supramolecular gelators. Langmuir 2010;26(8):5909-17.

[12] Luo M, Zhou X, Chi Z, Liu S, Zhang Y, Xu J. Fluorescence-enhanced organogelators with mesomorphic and piezofluorochromic properties based on tetraphenylethylene and gallic acid derivatives. Dyes and Pigments 2014;101:74-84.

[13] Luo M, Wang S, Wang M, Huang S, Li C, Chen L, et al. Novel organogel harnessing Excited-State Intramolecular Proton Transfer process with aggregation induced emission and photochromism. Dyes and Pigments 2016;132:48-57.

[14] Zhang C, Li Y, Xue X, Chu P, Liu C, Yang K, et al. A smart pH-switchable luminescent hydrogel. Chemical communications 2015;51(20):4168-71.

[15] Babu SS, Praveen VK, Ajayaghosh A. Functional pi-gelators and their applications. Chem Rev 2014;114(4):1973-2129.

[16] Zhang Q, Qu DH, Ma X, Tian H. Sol-gel conversion based on photoswitching between noncovalently and covalently linked netlike supramolecular polymers.

Chemical communications 2013;49(84):9800-2.

[17] Luo M, Zhou X, Chi Z, Ma C, Zhang Y, Liu S, et al. Synthesis and Properties of Gelators Derived from Tetraphenylethylene and Gallic Acid with Aggregation-Induced Emission. Journal of Molecular and Engineering Materials 2013;01(03):1340007.

[18] Yang X, Zhang G, Zhang D. Stimuli responsive gels based on low molecular weight gelators. J Mater Chem 2012;22(1):38-50.

[19] Sun F, Zhang G, Zhang D. A new gelator based on tetraphenylethylene and diphenylalanine: Gel formation and reversible fluorescence tuning. Chin Sci Bull 2012;57(33):4284-8.

[20] Zhang P, Wang H, Liu H, Li M. Fluorescence-enhanced organogels and mesomorphic superstructure based on hydrazine derivatives. Langmuir 2010;26(12):10183-90.

[21] Nayak MK, Kim B-H, Kwon JE, Park S, Seo J, Chung JW, et al. Gelation-Induced Enhanced Fluorescence Emission from Organogels of Salicylanilide-Containing Compounds Exhibiting Excited-State Intramolecular Proton Transfer: Synthesis and Self-Assembly. Chemistry - A European Journal 2010;16(25):7437-47.

[22] Chen Q, Zhang D, Zhang G, Yang X, Feng Y, Fan Q, et al. Multicolor Tunable Emission from Organogels Containing Tetraphenylethene, Perylenediimide, and Spiropyran Derivatives. Adv Funct Mater 2010;20(19):3244-51.

[23] Simalou O, Zhao X, Lu R, Xue P, Yang X, Zhang X. Strategy to control the

chromism and fluorescence emission of a perylene dye in composite organogel phases. Langmuir 2009;25(19):11255-60.

[24] Chen P, Lu R, Xue P, Xu T, Chen G, Zhao Y. Emission enhancement and chromism in a salen-based gel system. Langmuir 2009;25(15):8395-9.

[25] An B-K, Lee D-S, Lee J-S, Park Y-S, Song H-S, Park SY. Strongly Fluorescent Organogel System Comprising Fibrillar Self-Assembly of a Trifluoromethyl-Based Cyanostilbene Derivative. J Am Chem Soc 2004;126:10232-3.

[26] Xue P, Lu R, Lu R, Zhang Y, Nomoto H, Takafuji M, et al. Functional organogel based on a salicylideneaniline derivative with enhanced fluorescence emission and photochromism. Chem Eur J 2007;13(29):8231-9.

[27] Arumugaperumal R, Raghunath P, Lin M, Chung W. Distinct Nanostructures and Organogel Driven by Reversible Molecular Switching of a Tetraphenylethene-Involved Calix[4]arene-Based Amphiphilic [2]Rotaxane. Chem Mater 2018;30:7221-33.

[28] Wu J, Yi T, Shu T, Yu M, Zhou Z, Xu M, et al. Ultrasound Switch and Thermal Self-Repair of Morphology and Surface Wettability in a Cholesterol-Based Self-Assembly System. Angew Chem 2008;120(6):1079-83.

[29] Wu J, Yi T, Xia Q, Zou Y, Liu F, Dong J, et al. Tunable gel formation by both sonication and thermal processing in a cholesterol-based self-assembly system. Chem Eur J 2009;15(25):6234-43.

[30] Yang XL, Liu YJ, Li JH, Wang Q, Yang M, Li C. A novel aggregation-induced-emission-active supramolecular organogel for the detection of

volatile acid vapors. New J Chem 2018;42(21):17524-32.

[31] Wang H LQ, Hu Y, Liu M, Huang X, Gao W, Wu H,. A Multiple Stimuli-Sensitive Low-Molecular-Weight Gel with an Aggregate-Induced Emission Effect for Sol–Gel Transition Detection. ChemistryOpen 2018;7:457-62.

[32] Bardelang D. Ultrasound induced gelation: a paradigm shift. Soft Matter 2009;5(10):1969.

[33] Naito M, Inoue R, Iida M, Kuwajima Y, Kawamorita S, Komiya N, et al. Control of Metal Arrays Based on Heterometallics Masquerading in Heterochiral Aggregations of Chiral Clothespin-Shaped Complexes. Chemistry 2015;21(37):12927-39.

[34] Isozaki K, Takaya H, Naota T. Ultrasound-induced gelation of organic fluids with metalated peptides. Angew Chem Int Ed Engl 2007;46(16):2855-7.

[35] Nuthanakanti A, Srivatsan SG. Hierarchical self-assembly of switchable nucleolipid supramolecular gels based on environmentally-sensitive fluorescent nucleoside analogs. Nanoscale 2016;8(6):3607-19.

[36] Shen J, Ding P, Gao L, Gao Y, Zhang Q, Yuan S, Xin X. Formation of organogels with aggregation-induced emission characteristics triggered by thermal and ultrasound. Colloid Polym Sci 2017;295:1765-72.

[37] Yan D, Tang Y, Lin H, Wang D. Tunable two-color luminescence and host-guest energy transfer of fluorescent chromophores encapsulated in metal-organic frameworks. Scientific reports 2014;4:4337.

[38] Xu B, Chi Z, Zhang J, Zhang X, Li H, Li X, et al. Piezofluorochromic and

aggregation-induced-emission compounds containing triphenylethylene and tetraphenylethylene moieties. Chem Asian J 2011;6(6):1470-8.

[39] Zhang X, Chi Z, Li H, Xu B, Li X, Liu S, et al. Synthesis and properties of novel aggregation-induced emission compounds with combined tetraphenylethylene and dicarbazolyl triphenylethylene moieties. J Mater Chem 2011;21(6):1788-96.

[40] Xu B, Chi Z, Li H, Zhang X, Li X, Liu S, et al. Synthesis and Properties of Aggregation-Induced Emission Compounds Containing Triphenylethene and Tetraphenylethene Moieties. The Journal of Physical Chemistry C 2011;115(35):17574-81.

[41] Chung JW, An B-K, Park SY. A Thermoreversible and Proton-Induced Gel-Sol Phase Transition with Remarkable Fluorescence Variation. Chem Mater 2008;20:6750–5.

[42] Zhu L, Ma X, Ji F, Wang Q, Tian H. Effective enhancement of fluorescence signals in rotaxane-doped reversible hydrosol-gel systems. Chemistry 2007;13(33):9216-22.

[43] Hanabusa K, Matsumoto M, Kimura M, Kakehi A, Shirai H. Low Molecular Weight Gelators for Organic Fluids: Gelation Using a Family of Cyclo(dipeptide)s. J Colloid Interface Sci 2000;224(2):231-44.

[44] Estroff L, Leiserowitz L, Addadi L, Weiner S, Hamilton A. Characterization of an organic hydrogel: a cryo‐transmission electron microscopy and X‐ray diffraction study. Adv Mater 2003;15:38-42.

Table 1 Gelation properties in various solvents

Solvents	Phase	Solvents	Phase
Cyclohexane	G	Toluene	S
DMF	S	Chloroform	S
DMSO	S	Hexane	I
p-Xylele	S	Petroleum ether	I
1,4-Dioxane	S	Ethanol	I
Actonitrile	PG	THF	S
Ethyl acetate	S	Dichloromethane	S
Actone	S	Ethylene glycol	S
Diethyl ether	S	Methyl alcohol	I

G: stable gel formed at room temperature; PG: partial gel; S: soluble; I: insoluble; P: precipitate.

Table 2. the CGC and Tg of S-gel and T-gel in cyclohexane solvent

	CGC(mg mL^{-1})	T$_g$ (^{o} C)
S-gel	17	65~68
T-gel	60	62~66

Table 3 The wavelengths of the IR band related to amide and ester groups of TPE-Ch before gel and after gel.

	υ_{NH} (cm^{-1})	$\upsilon_{C=O}$ (cm^{-1})
Before gel	3413	1733
S-gel	3433,3343,1670	1733
T-gel	3331,1671	1733
R-gel	3331,1671	1733

Figure captions

Figure 1 (A) PL spectra of **TPE-Ch** in THF/water mixtures with different water fractions (Inset: Change in PL peak intensities with different water fractions in THF/water mixtures, concentration 2.5 × 10^{-5}M, λ_{em} = 474 nm), (B) the images in THF/water mixtures with different water fractions were taken under room light (top) and 300 nm UV light (bottom).

Figure 2 Molecular orbital amplitude plots of HOMO and LUMO energy levels of **TPE-Ch**.

Figure 3 Pictures of S-gel (55.8 mg mL^{-1}, ultrasonic treatment: 200 W, 53 kHz, 5 minutes); T-gel (133.4 mg mL^{-1}); and R-gel (55.8 mg mL^{-1}) in cyclohexane: under room light (left) and 365 nm UV light (right).

Figure 4 the relationship between the power and the time needed to form S-gel in different concentration.

Figure 5 (A) the emission images in sol (left) and gel (right) state under room light (top) and 365 nm UV light (bottom), (B) Temperature-dependent fluorescence spectra in cyclohexane (60 mg/ml, λ_{ex} = 365 nm).

Figure 6 （A）SEM images of the xerogels from the **TPE-Ch** in S-gel (55.8 mg mL^{-1}, ultrasonic treatment: 200 W, 53 kHz, 5 minutes); T-gel (133.4 mg mL^{-1}); and R- gel (55.8 mg mL^{-1}).（B）AFM image of xerogel in S-gel (55.8 mg mL^{-1}), (C) TEM image of xerogel in T-gel (114 mg mL^{-1}).

Figure 7 Normalized fluorescent spectra of **TPE-Ch** in S-gel (55.8 mg mL^{-1}, ultrasonic treatment: 200 W, 53 kHz, 5 minutes); T-gel (133.4 mg mL^{-1}); and R- gel

(55.8 mg mL^{-1}).

Figure 8 IR spectra for xerogel of **TPE-Ch** in S-gel (55.8 mg mL^{-1}, ultrasonic treatment: 200 W, 53 kHz, 5 minutes); T-gel (133.4 mg mL^{-1}); and R- gel (55.8 mg mL^{-1}).

Figure 9 Powder XRD profile of the neat solid and xerogel of **TPE-Ch** at room temperature: (A) Small angle X-ray diffraction (SAXD), (B) Wide angle X-ray diffraction (WAXD).

Figure 10 Perspective structures of **TPE-Ch**; structure A: isolated **TPE-Ch**; structure B: aggregation in the T-gel; structure C: aggregation in the S-gel; White C, red O, blue N.

Figure 11 DSC curves of compound **TPE-Ch.**

Figure 12 Optical micrographs of compound **TPE-Ch** between crossed polarizers: liquid crystalline texture at 140 °C.

Figure 13 TGA thermograms of TPE-Ch.

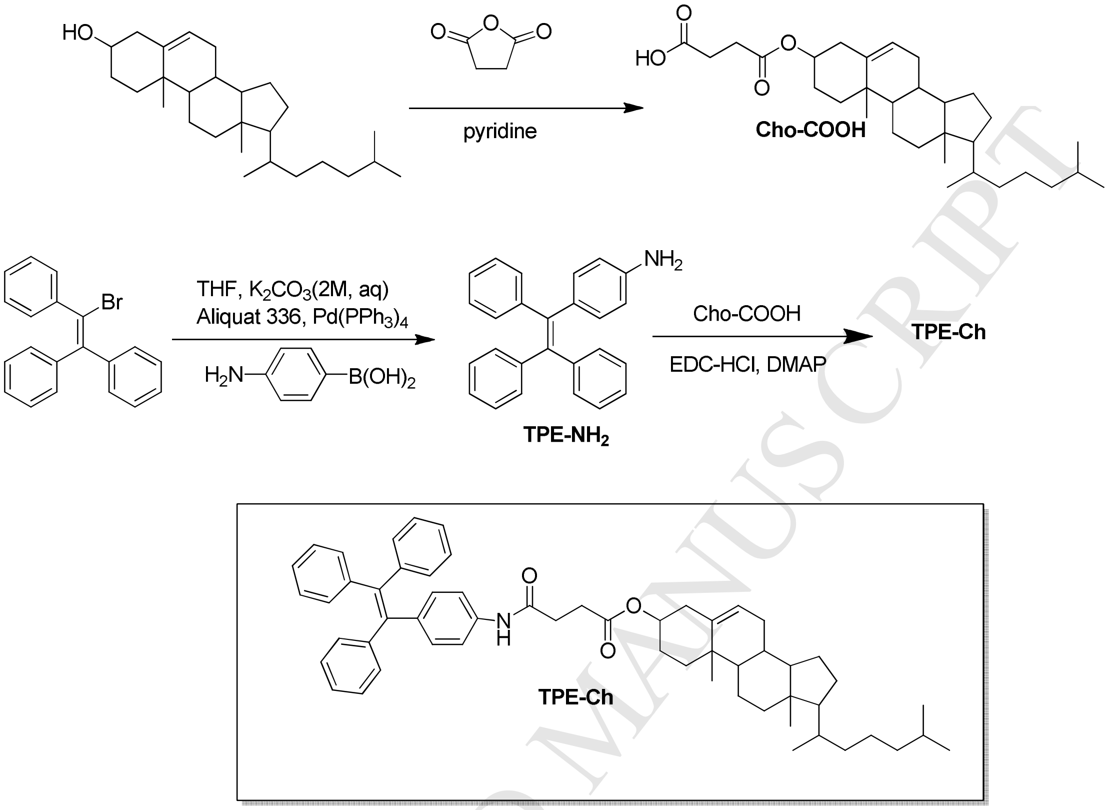

Scheme 1

Scheme 1 Synthetic routes for **TPE-Ch**

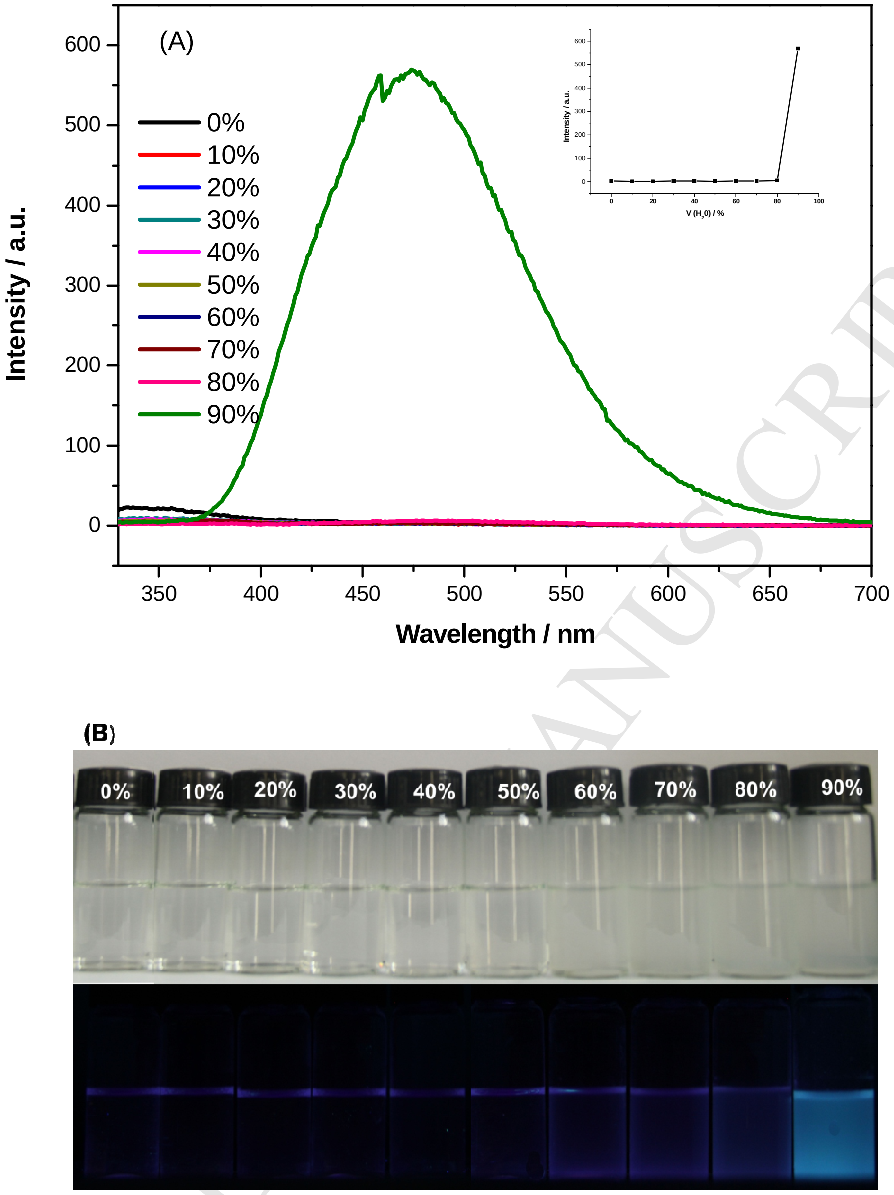
(A)
Intensity / a.u.
Wavelength / nm
0
100
200
300
400
500
600
350
400
450
500
550
600
650
700
0%
10%
20%
30%
40%
50%
60%
70%
80%
90%
Intensity / a.u.
V (H2O) / %
0
20
40
60
80
100
(B)
0%
10%
20%
30%
40%
50%
60%
70%
80%
90%

Figure 1

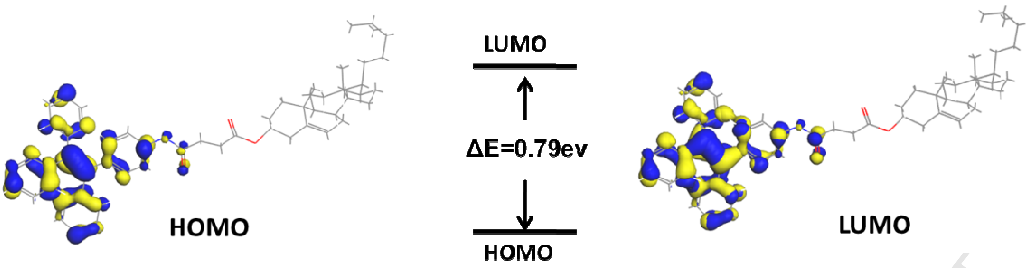

Figure 2

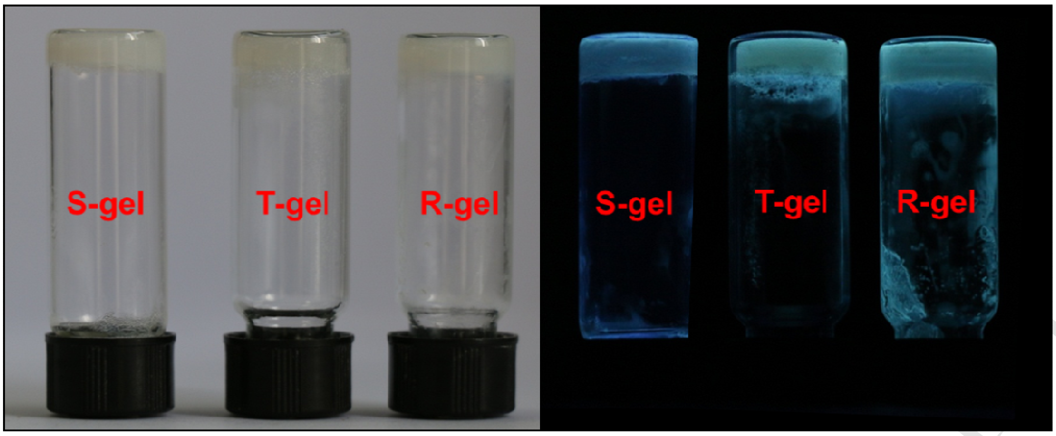

Figure 3

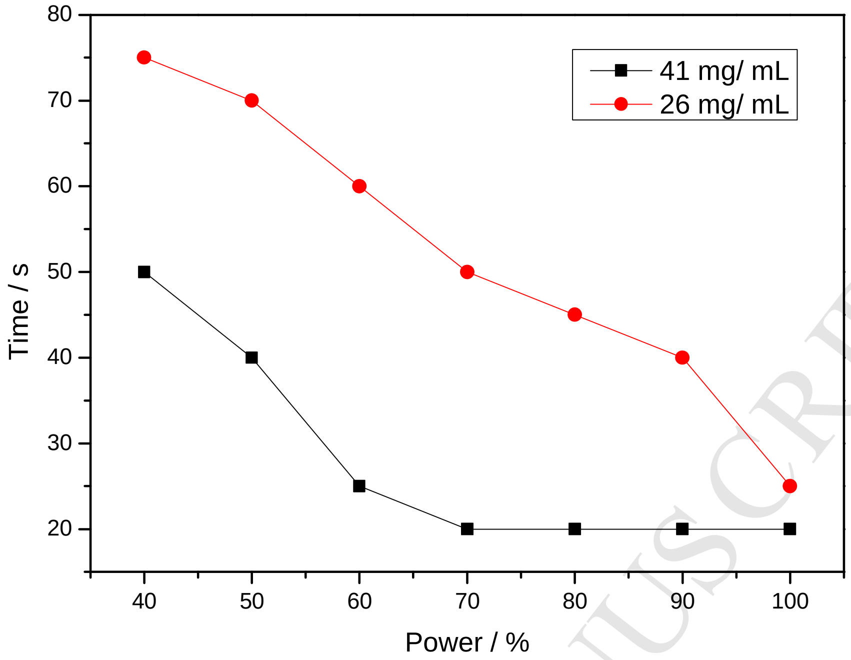
Time / s
Power / %
80
70
60
50
40
30
20
40
50
60
70
80
90
100
41 mg/ mL
26 mg/ mL

Figure 4

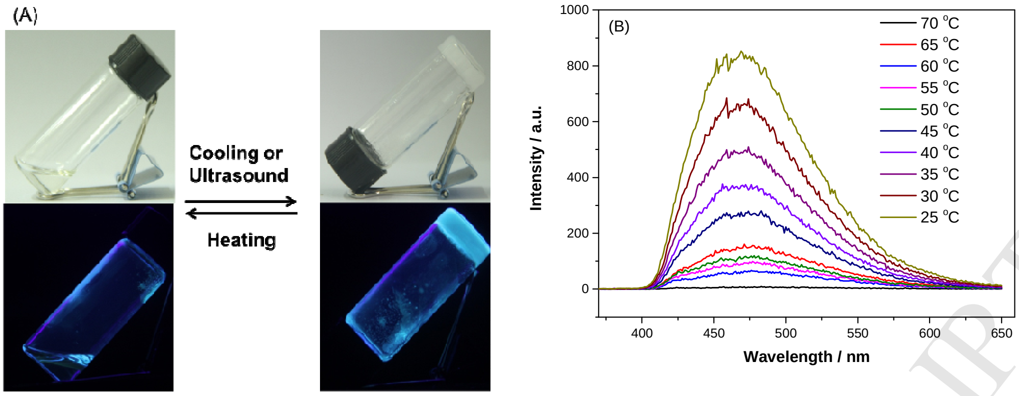
(A)
Cooling or Ultrasound
Heating
(B)
Intensity / a.u.
Wavelength / nm
0
200
400
600
800
1000
400
450
500
550
600
650
70 °C
65 °C
60 °C
55 °C
50 °C
45 °C
40 °C
35 °C
30 °C
25 °C

Figure 5

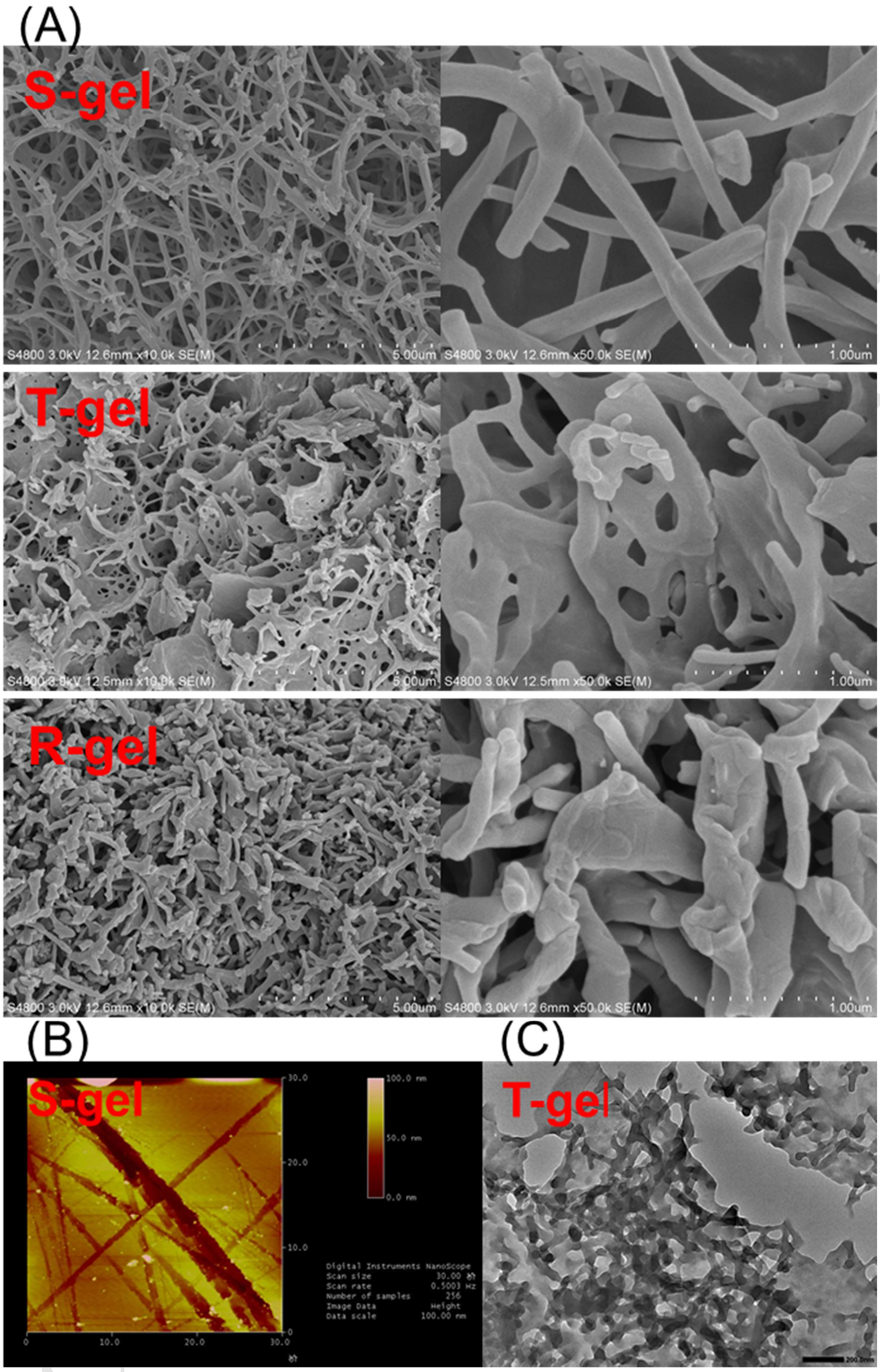
(A)
S-gel
S4800 3.0kV 12.6mm x10.0k SE(M)
5.00um
S4800 3.0kV 12.6mm x50.0k SE(M)
1.00um
T-gel
S4800 3.0kV 12.5mm x10.0k SE(M)
5.00um
S4800 3.0kV 12.5mm x50.0k SE(M)
1.00um
R-gel
S4800 3.0kV 12.6mm x10.0k SE(M)
5.00um
S4800 3.0kV 12.6mm x50.0k SE(M)
1.00um
(B)
S-gel
30.0
20.0
10.0
0
10.0
20.0
30.0
µm
100.0 nm
50.0 nm
0.0 nm
Digital Instruments NanoScope
Scan size 30.00 µm
Scan rate 0.5003 Hz
Number of samples 256
Image Data Height
Data scale 100.00 nm
(C)
T-gel
200.0nm

Figure 6

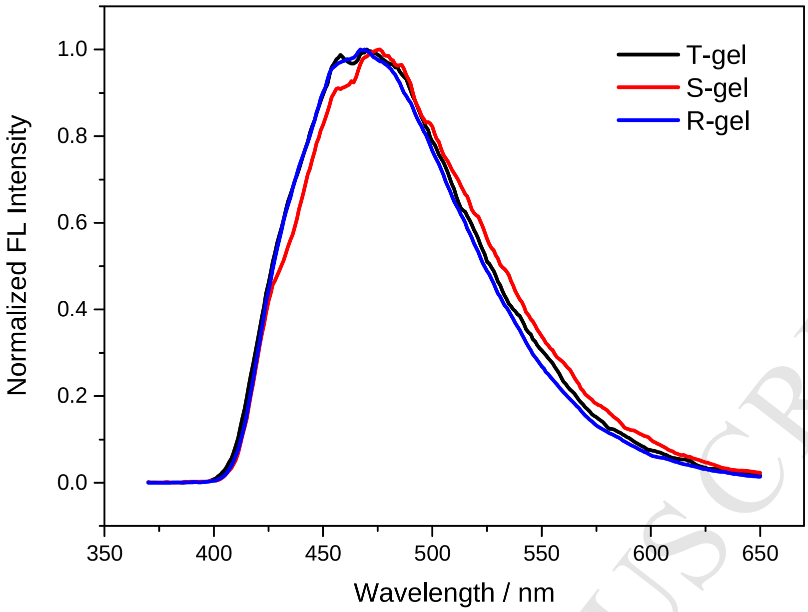

Normalized FL Intensity
1.0
0.8
0.6
0.4
0.2
0.0
350
400
450
500
550
600
650
Wavelength / nm
T-gel
S-gel
R-gel

Figure 7

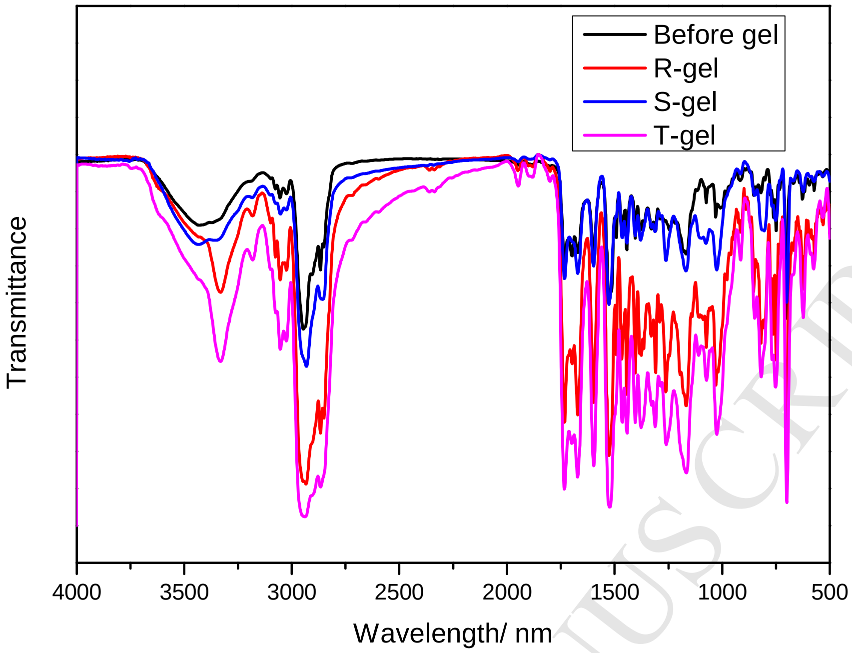
Before gel
R-gel
S-gel
T-gel
Transmittance
4000
3500
3000
2500
2000
1500
1000
500
Wavelength/ nm

Figure 8

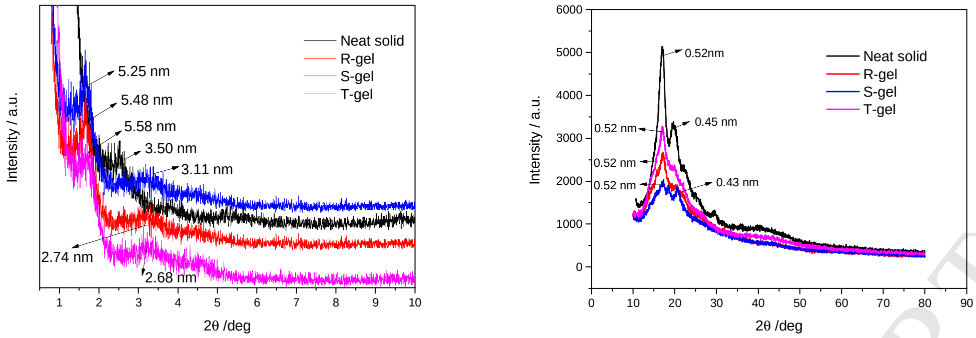
Intensity / a.u.
2θ /deg
Neat solid
R-gel
S-gel
T-gel
5.25 nm
5.48 nm
5.58 nm
3.50 nm
3.11 nm
2.74 nm
2.68 nm
1
2
3
4
5
6
7
8
9
10
Intensity / a.u.
2θ /deg
0
1000
2000
3000
4000
5000
6000
0
10
20
30
40
50
60
70
80
90
0.52nm
0.45 nm
0.52 nm
0.52 nm
0.52 nm
0.43 nm
Neat solid
R-gel
S-gel
T-gel

Figure 9

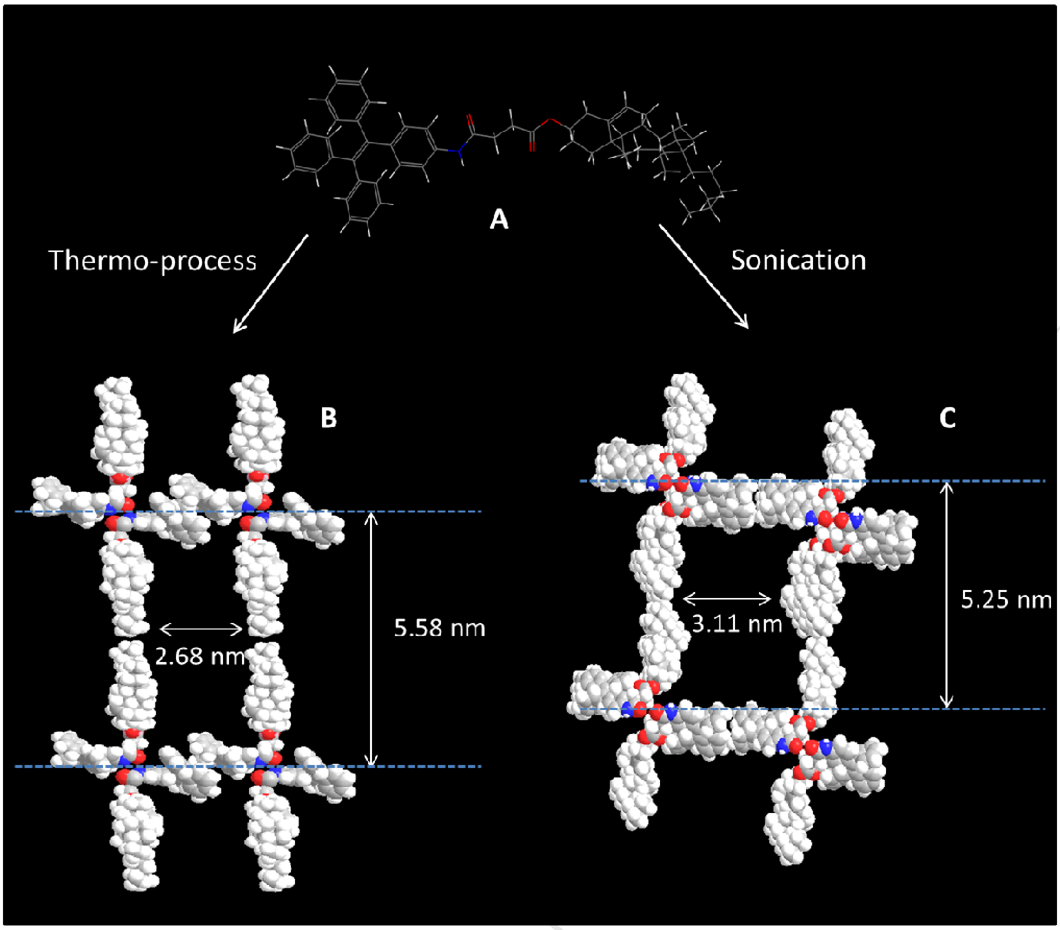

Figure 10

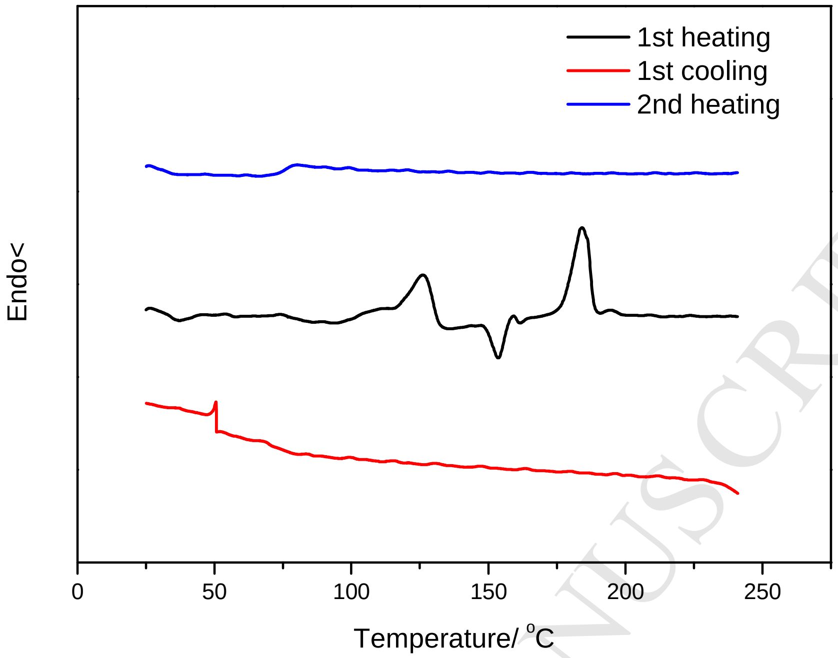
1st heating
1st cooling
2nd heating
Endo<
0
50
100
150
200
250
Temperature/ °C

Figure 11

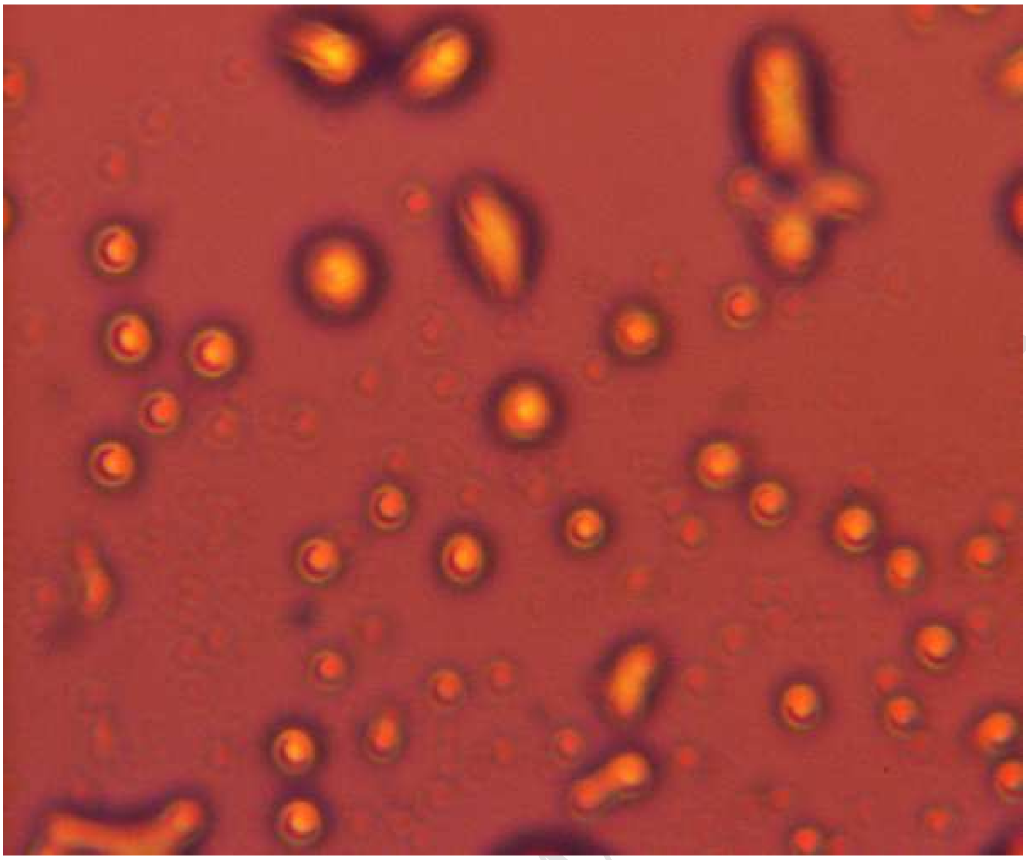

Figure 12

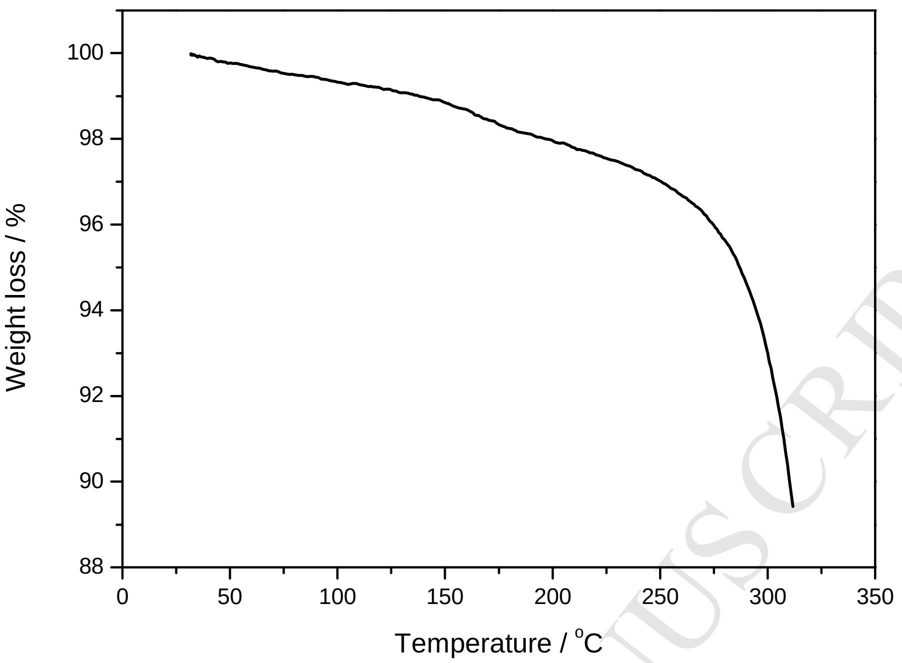
Weight loss / %
100
98
96
94
92
90
88
0
50
100
150
200
250
300
350
Temperature / ^{o}C

Figure 13

Supporting Information

Aggregation-induced emission organogel formed by both sonication and thermal processing based on tetraphenylethylene and cholesterol derivative

Miao Luo,[a] Sheng Wang,*[a] Chengpeng Li,[a] Wangen Miao,[a] and Xiang Ma*[b]

[a]*College of Basic Education, School of Chemistry and Chemical Engineering, Lingnan Normal University, Zhanjiang Preschool Education College, Zhanjiang, 524037, Guangdong, P. R. China.*
[b]*Key Laboratory for Advanced Materials and Institute of Fine Chemicals, East China University of Science & Technology, Shanghai 200237, P. R. China.*

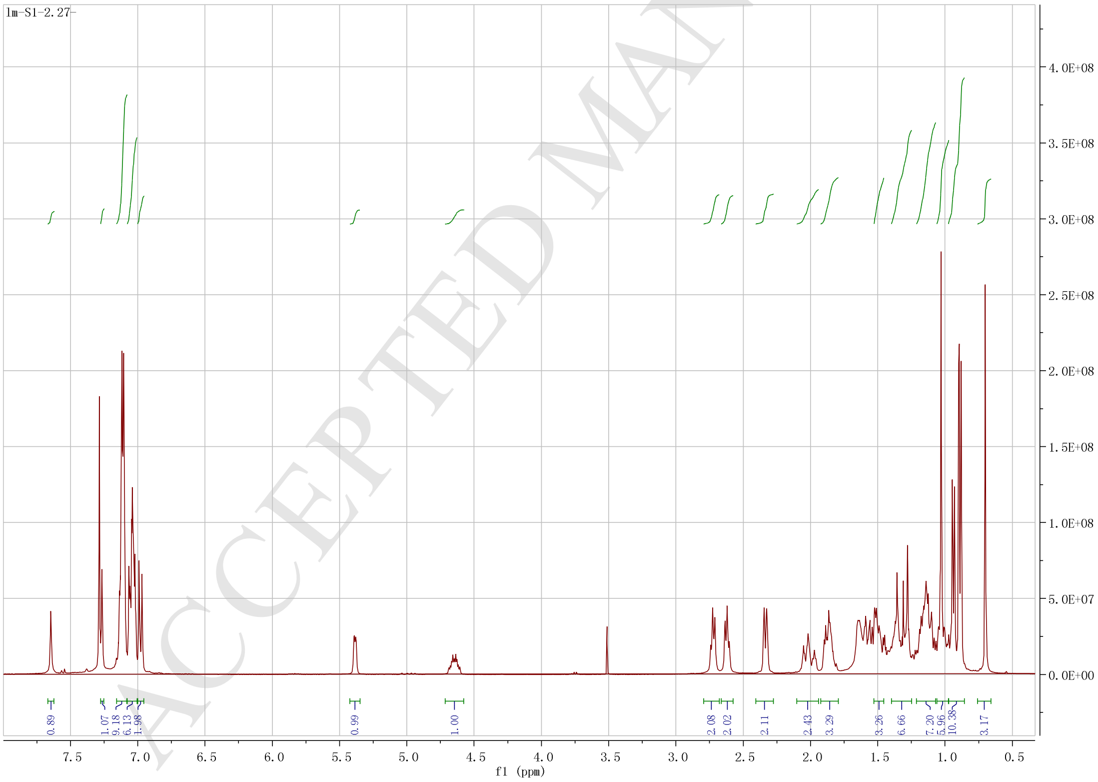

^{1}HNMR

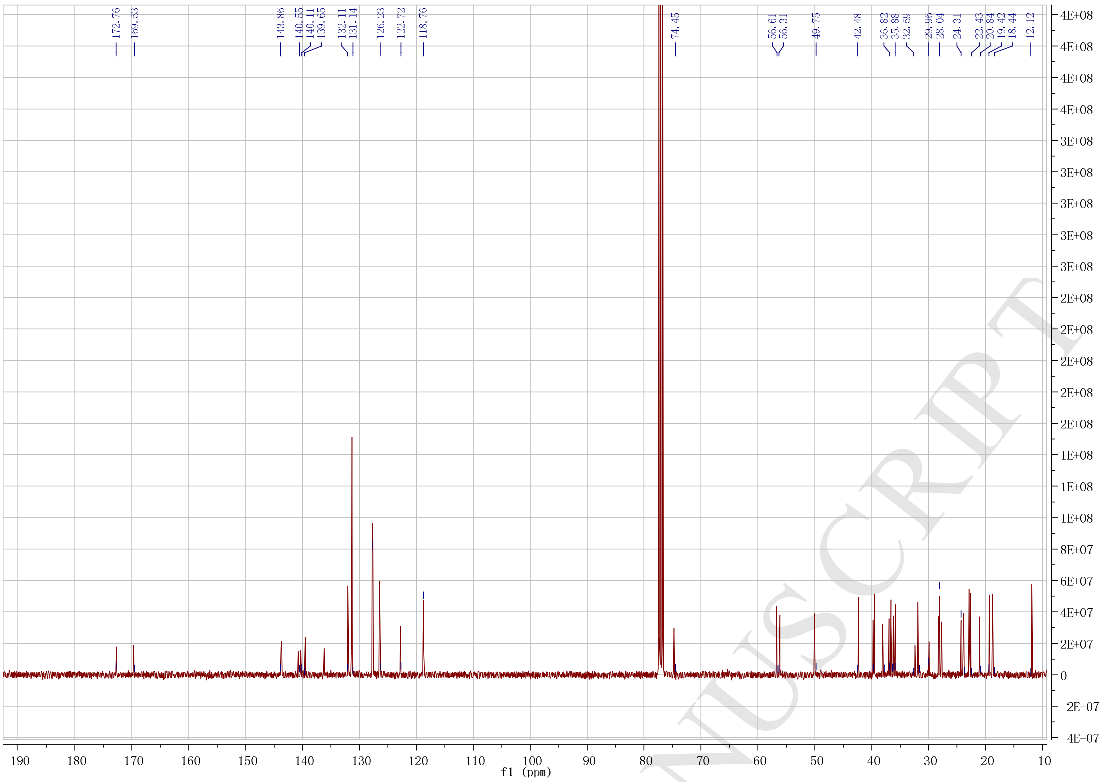

^{13}CNMR

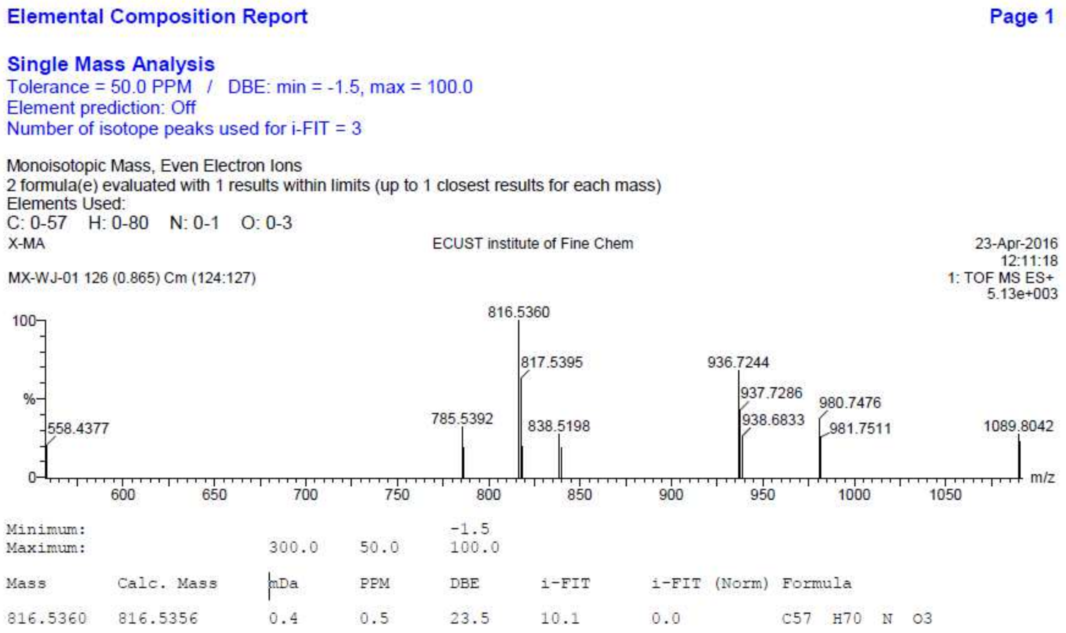

Elemental Composition Report **Page 1**

Single Mass Analysis
Tolerance = 50.0 PPM / DBE: min = -1.5, max = 100.0
Element prediction: Off
Number of isotope peaks used for i-FIT = 3

Monoisotopic Mass, Even Electron Ions
2 formula(e) evaluated with 1 results within limits (up to 1 closest results for each mass)
Elements Used:
C: 0-57 H: 0-80 N: 0-1 O: 0-3
X-MA ECUST institute of Fine Chem 23-Apr-2016
12:11:18
MX-WJ-01 126 (0.865) Cm (124:127) 1: TOF MS ES+
5.13e+003

```
Minimum:                                  -1.5
Maximum:                  300.0     50.0   100.0

Mass      Calc. Mass     mDa     PPM     DBE      i-FIT     i-FIT (Norm) Formula

816.5360  816.5356       0.4     0.5     23.5     10.1      0.0          C57  H70  N  O3
```

MS

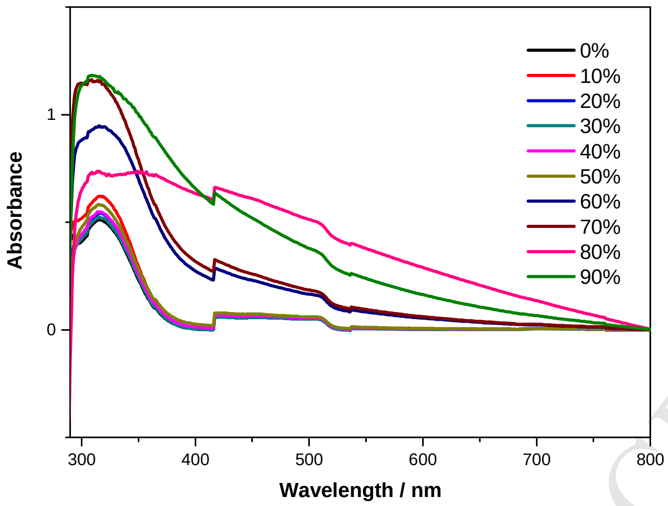

Figure S1. UV absorption spectra in THF/water mixtures with different volume.

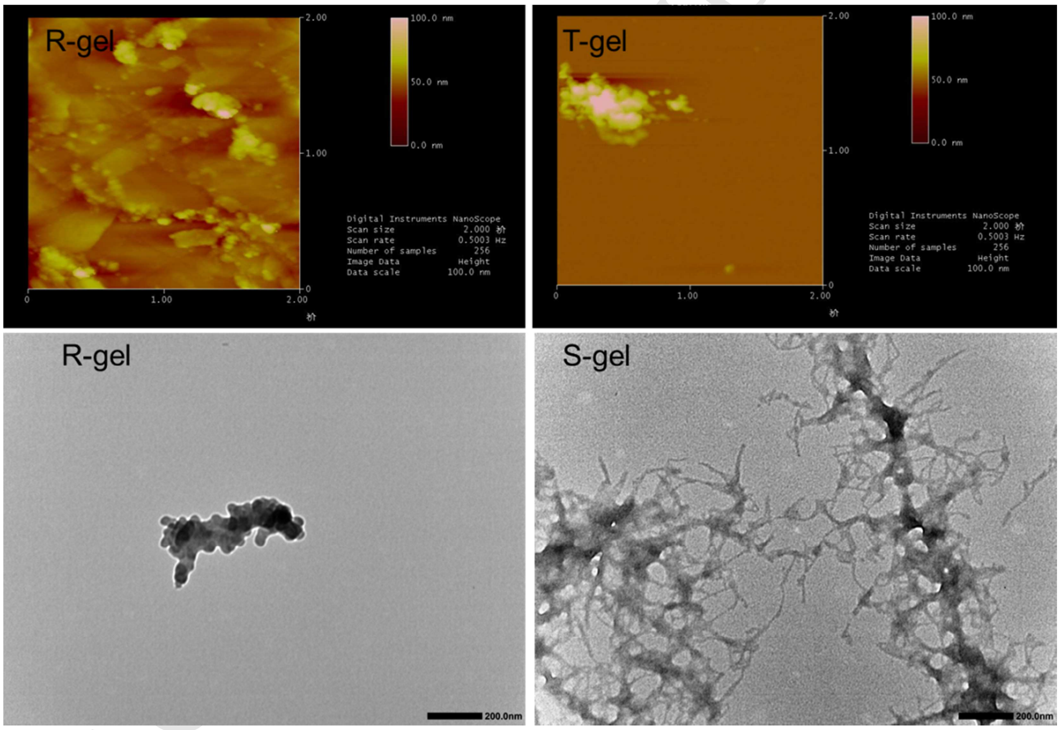

Figure S2. AFM image of xerogel in R-gel (55.8 mg mL^{-1}) and T-gel (133 mg mL^{-1}), (c) TEM image of xerogel in S-gel (26 mg mL^{-1})and R-gel (26 mg mL^{-1}).

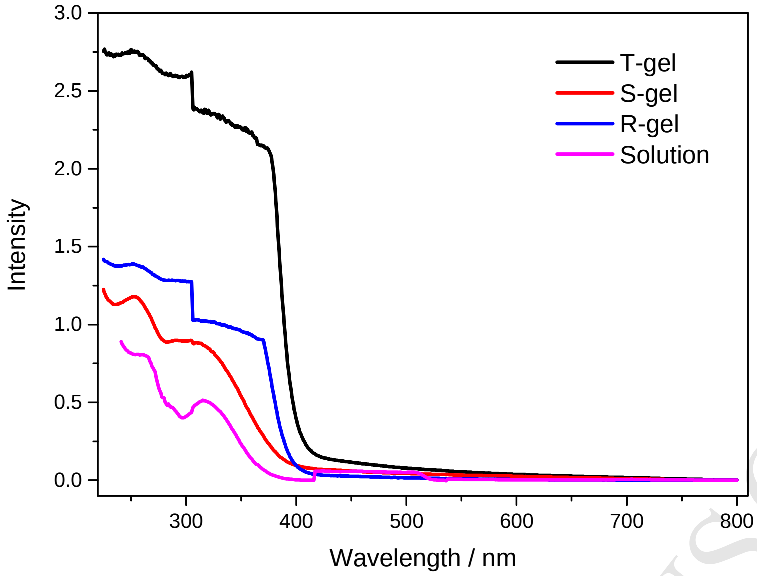

Figure S3. Absorption spectra of **TPE-Ch** in THF solution (2.5×10^{-5} mol L^{-1}), S-gel (55.8 mg mL^{-1}, ultrasonic treatment: 200 W, 53 kHz, 5 minutes); T-gel (133.4 mg mL^{-1}); and R- gel (55.8 mg mL^{-1}).

Aggregation-induced emission organogel formed by both sonication and thermal processing based on tetraphenylethylene and cholesterol derivative

Miao Luo,[a] Sheng Wang,*[a] Chengpeng Li,[a] Wangen Miao,[a] and Xiang Ma*[b]

Highlights

- A novel asymmetric tetraphenylethylene-based fluorescence compound was synthesized.
- The compound can form cholesteryl liquid crystal by cooling from the isotropic melt.
- The compound could gelate in cyclohexane exhibiting enhanced emission via both ultrasound stimuli and general sol–gel processes.